ESAIM: PROCEEDINGS AND SURVEYS, September 2024, Vol. 76, p.20-34
Gloria Faccanoni, Bérénice Grec, Olivier Hurisse, Jonathan Jung, Hélène Mathis

IMPROVED CROUZEIX-RAVIART SCHEME FOR THE STOKES AND NAVIER-STOKES PROBLEM

Eric Chénier[1], Erell Jamelot[2], Christophe Le Potier[3] and Andrew Peitavy[4]

Abstract. The resolution of the incompressible Navier-Stokes equations is tricky, and it is well known that one of the major issue is to approach the space:

$$\mathbf{H}^1(\Omega) \cap \mathbf{H}(\operatorname{div} 0;\Omega) := \left\{ \mathbf{v} \in \mathbf{H}^1(\Omega) \ : \ \operatorname{div} \mathbf{v} = 0 \right\}.$$

The non-conforming Crouzeix-Raviart finite e lement a re c onvenient s ince t hey i nduce l ocal mass conservation. Moreover they are such that the stability constant of the Fortin operator is equal to 1. This implies that they can easily handle anisotropic mesh [1, 2]. However spurious velocities may appear and damage the approximation.

We propose a scheme here that allows one to reduce the spurious velocities. It is based on a new discretisation for the gradient of pressure based on the symmetric MPFA scheme (finite volume MultiPoint Flux Approximation) [3, 4, 5].

1. Motivation

The TrioCFD [6] code is a computational fluid d ynamics (CFD) s imulation s oftware d eveloped a t the CEA. It is open source, object-oriented and massively parallel. It is dedicated to the numerical simulation of turbulent flows for scientific and industrial applications, particularly in the nuclear fie ld. Let Ω, the domain of study, be an open connected bounded domain of $\mathbb{R}^d$, $d = 2, 3$, with a polygonal ($d = 2$) or Lipschitz polyhedral ($d = 3$) boundary $\partial\Omega$ with constant physical properties. Let $T > 0$ be a simulation time. The TrioCFD code solves the incompressible Navier-Stokes equations which read: Find $(\mathbf{u}(\mathbf{x},t), p(\mathbf{x},t))$ such that $\forall (\mathbf{x},t) \in \Omega \times (0,T)$,

$$\left\{ \begin{array}{rcl} \partial_t \mathbf{u} - \nu \boldsymbol{\Delta}\, \mathbf{u} + (\mathbf{u} \cdot \mathbf{grad}\,)\mathbf{u} + \mathbf{grad}\, p &=& \mathbf{f}, \\ \operatorname{div} \mathbf{u} &=& 0, \\ u(\mathbf{x},0) &=& u_0(\mathbf{x}). \end{array} \right. \tag{1}$$

We consider here Dirichlet boundary conditions for the velocity $\mathbf{u}$ and we impose a normalization condition for the pressure p:

$$\mathbf{u} = 0 \text{ on } \partial\Omega, \quad \int_\Omega p = 0.$$

The vector field $\mathbf{u}$ represents the velocity of the fluid and the scalar field p represents its pressure divided by the fluid density which is supposed to be constant. The first equation of (1) corresponds to the momentum balance equation and the second one corresponds to the mass conservation. The constant parameter $\nu > 0$ is the kinematic viscosity of the fluid. The vector field $\mathbf{f}$ represents the body force divided by the fluid density. We first consider the steady Stokes problem which reads:

$$\text{Find } (\mathbf{u}, p) \text{ such that } \forall \mathbf{x} \in \Omega : \left\{ \begin{array}{rcl} -\nu \Delta \mathbf{u} + \mathbf{grad}\, p &=& \mathbf{f}, \\ \operatorname{div} \mathbf{u} &=& 0. \end{array} \right. \tag{2}$$

[1] Univ Gustave Eiffel, Univ Paris Est Creteil, CNRS, UMR 8208, MSME, F-77454 Marne-la-Vallée, France. eric.chenier@univ-eiffel.fr

[2] Université Paris-Saclay, CEA, Service de Thermo-hydraulique et de Mécanique des Fluides, 91191 Gif-sur-Yvette, France. erell.jamelot@cea.fr

[3] Université Paris-Saclay, CEA, Service de Thermo-hydraulique et de Mécanique des Fluides, 91191 Gif-sur-Yvette, France. christophe.le-potier@cea.fr

[4] Université Paris-Saclay, CEA, Service de Thermo-hydraulique et de Mécanique des Fluides, 91191 Gif-sur-Yvette, France. andrew.peitavy@cea.fr

Article published online by EDP Sciences and available at https://www.esaim-proc.org or https://doi.org/10.1051/proc/202476020

Before stating the variational formulation of Problem (2), we provide some definitions and reminders. Let us set $\mathbf{L}^2(\Omega) = (L^2(\Omega))^d$, $\mathbf{H}^1_0(\Omega) = (H^1_0(\Omega))^d$, $\mathbf{H}^{-1}(\Omega) = (H^{-1}(\Omega))^d$ its dual space and $L^2_{zmv}(\Omega) = \{q \in L^2(\Omega) \,|\, \int_\Omega q = 0\}$. We recall that $\mathbf{H}(\mathrm{div}\,;\Omega) = \{\mathbf{v} \in \mathbf{L}^2(\Omega) \,|\, \mathrm{div}\,\mathbf{v} \in L^2(\Omega)\}$. Let us first recall Poincaré-Steklov inequality:

$$\exists C_{PS} > 0 \,|\, \forall v \in H^1_0(\Omega), \quad \|v\|_{L^2(\Omega)} \leq C_{PS} \|\mathbf{grad}\, v\|_{\mathbf{L}^2(\Omega)}. \tag{3}$$

Thanks to this result, in $H^1_0(\Omega)$, the semi-norm is equivalent to the natural norm, so that the scalar product reads $(v,w)_{H^1_0(\Omega)} = (\mathbf{grad}\, v, \mathbf{grad}\, w)_{\mathbf{L}^2(\Omega)}$ and the norm is $\|v\|_{H^1_0(\Omega)} = \|\mathbf{grad}\, v\|_{\mathbf{L}^2(\Omega)}$. Let $\mathbf{v}$, $\mathbf{w} \in \mathbf{H}^1_0(\Omega)$, we denote by $(v_i)_{i=1}^d$ (resp. $(w_i)_{i=1}^d$) the components of $\mathbf{v}$ (resp. $\mathbf{w}$), and we set $\mathbf{Grad}\,\mathbf{v} = (\partial_j v_i)_{i,j=1}^d \in \mathbb{L}^2(\Omega)$, where $\mathbb{L}^2(\Omega) = [L^2(\Omega)]^{d\times d}$. We have:

$$(\mathbf{Grad}\,\mathbf{v}, \mathbf{Grad}\,\mathbf{w})_{\mathbb{L}^2(\Omega)} = (\mathbf{v},\mathbf{w})_{\mathbf{H}^1_0(\Omega)} = \sum_{i=1}^d (v_i, w_i)_{H^1_0(\Omega)} \text{ and } \|\mathbf{v}\|_{\mathbf{H}^1_0(\Omega)} = \|\mathbf{Grad}\,\mathbf{v}\|_{\mathbb{L}^2(\Omega)}.$$

Let us set $\mathbf{V} = \left\{\mathbf{v} \in \mathbf{H}^1_0(\Omega) \,|\, \mathrm{div}\,\mathbf{v} = 0\right\}$. The space $\mathbf{V}$ is a closed subset of $\mathbf{H}^1_0(\Omega)$. We denote by $\mathbf{V}^\perp$ the orthogonal of $\mathbf{V}$ in $\mathbf{H}^1_0(\Omega)$. We recall that [7, cor. I.2.4]:

Proposition 1.1. *The operator* $\mathrm{div} : \mathbf{H}^1_0(\Omega) \to L^2(\Omega)$ *is an isomorphism of* $\mathbf{V}^\perp$ *onto* $L^2_{zmv}(\Omega)$. *We call* C_{div} *the constant such that:*

$$\forall p \in L^2_{zmv}(\Omega),\ \exists! \mathbf{v} \in \mathbf{V}^\perp \,|\, \mathrm{div}\,\mathbf{v} = p \text{ and } \|\mathbf{v}\|_{\mathbf{H}^1_0(\Omega)} \leq C_{\mathrm{div}}\, \|p\|_{L^2(\Omega)}. \tag{4}$$

Let us set :

$$a_\nu : \left\{ \begin{array}{rcl} \mathbf{H}^1_0(\Omega) \times \mathbf{H}^1_0(\Omega) & \to & \mathbb{R} \\ (\mathbf{u}', \mathbf{v}) & \mapsto & \nu\,(\mathbf{u}', \mathbf{v})_{\mathbf{H}^1_0(\Omega)} \end{array} \right. \text{ and } b : \left\{ \begin{array}{rcl} \mathbf{H}^1_0(\Omega) \times L^2_{zmv}(\Omega) & \to & \mathbb{R} \\ (\mathbf{v}, q) & \mapsto & (\mathrm{div}\,\mathbf{v}, q)_{L^2(\Omega)} \end{array} \right. . \tag{5}$$

Classically, the variational formulation of Problem (2) reads:

$$\text{Find } (\mathbf{u},p) \in \mathbf{H}^1_0(\Omega) \times L^2_{zmv}(\Omega) \,|\, \left\{ \begin{array}{rcll} a_\nu(\mathbf{u},\mathbf{v})_{\mathbf{H}^1_0(\Omega)} - b(\mathbf{v},p) & = & \langle \mathbf{f}, \mathbf{v}\rangle & \forall \mathbf{v} \in \mathbf{H}^1_0(\Omega), \\ b(\mathbf{u},q) & = & 0 & \forall q \in L^2_{zmv}(\Omega). \end{array} \right. \tag{6}$$

This saddle point problem is well-posed. Indeed, the bilinear form $a_\nu(\cdot,\cdot)$ is continuous and coercive. Moreover, the bilinear form $b(\cdot,\cdot)$ is continuous and due to Proposition 1.1, it satisfies the following inf-sup condition:

$$\exists C_{\mathrm{div}} > 0,\ \forall q \in L^2_{zmv}(\Omega)\backslash\{0\}, \quad \exists\, \mathbf{v}_q \in \mathbf{H}^1_0(\Omega)\backslash\{0\} \,|\, \quad \frac{b(\mathbf{v}_q, q)}{\|\mathbf{v}_q\|_{\mathbf{H}^1_0(\Omega)}\, \|q\|_{L^2(\Omega)}} \geq C_{\mathrm{div}}\,. \tag{7}$$

In TrioCFD code, the spatial discretization of Problem (2) is based on first order nonconforming Crouzeix-Raviart finite element method.
The outline of this article is as follows: in Section 2, we provide some notations for the discretization. Next, in Section 3, we recall the first order nonconforming finite element method, that we call the $\mathbf{P}^1_{nc} - P^0$ scheme. Then in Section 4, we describe the spatial discretization of TrioCFD code for simplicial meshes. We call this discretization the $\mathbf{P}^1_{nc} - (P^0 + P^1)$ scheme. This discretization is very precise (in the sense that it reduces spurious velocities introduced in Section 3) in $2D$. It is also precise in $3D$, except when the source term is a strong gradient. In order to obtain the same accuracy in $3D$ than in $2D$, one must increase the number of degrees of freedom of the discrete pressure space, which leads to a more expensive numerical scheme. Our aim is to develop a new numerical scheme that would be precise both in $2D$ and $3D$, but at a lower cost. We present such a scheme in Section 5 and numerical illustrations in Section 6 and 7.

2. Discrete notations

We call $(O, (x_{d'})_{d'=1}^d)$ the Cartesian coordinates system, of orthonormal basis $(\boldsymbol{e}_{d'})_{d'=1}^d$. Consider $(\mathcal{T}_h)_h$ a simplicial triangulation sequence of Ω. For a triangulation $\mathcal{T}_h$, we use the following index sets:

- $\mathcal{I}_K$ denotes the index set of the elements, such that $\mathcal{T}_h := \bigcup_{\ell \in \mathcal{I}_K} K_\ell$ is the set of elements.
- $\mathcal{I}_F$ denotes the index set of the facets[1], such that $\mathcal{F}_h := \bigcup_{f \in \mathcal{I}_F} F_f$ is the set of facets.

[1]The term facet stands for face (resp. edge) when $d = 3$ (resp. $d = 2$).

Let $\mathcal{I}_F = \mathcal{I}_F^i \cup \mathcal{I}_F^b$, where $\forall f \in \mathcal{I}_F^i$, $F_f \subset \Omega$ and $\forall f \in \mathcal{I}_F^b$, $F_f \subset \partial\Omega$.
- $\mathcal{I}_S$ denotes the index set of the vertices, such that $(S_j)_{j\in\mathcal{I}_S}$ is the set of vertices.
Let $\mathcal{I}_S = \mathcal{I}_S^i \cup \mathcal{I}_S^b$, where $\forall j \in \mathcal{I}_S^i$, $S_j \subset \Omega$ and $\forall j \in \mathcal{I}_S^b$, $S_j \subset \partial\Omega$.

We also define the following index subsets:

- $\forall \ell \in \mathcal{I}_K$, $\mathcal{I}_{F,\ell} = \{f \in \mathcal{I}_F \,|\, F_f \subset K_\ell\}$, $\quad \mathcal{I}_{S,\ell} = \{j \in \mathcal{I}_S \,|\, S_j \subset K_\ell\}$.
- $\forall j \in \mathcal{I}_S$, $\mathcal{I}_{K,j} = \{\ell \in \mathcal{I}_K \,|\, S_j \subset K_\ell\}$, $\quad N_{K,j} := \mathrm{card}(\mathcal{I}_{K,j})$.
- For $d = 2$, we set: $\mathcal{I}_{S,i} = \{k \in \mathcal{I}_S \,|\, \exists f \in \mathcal{I}_F,\, F_f = S_k S_i\}$

Notice that in $2D$, $N_{K,j} = N_{S,j}$.
For all $f \in \mathcal{I}_F$, M_f denotes the barycentre of F_f, and by $\mathbf{n}_f$ a unit normal (outward oriented if $F_f \subset \partial\Omega$).
For all $j \in \mathcal{I}_S$, for all $\ell \in \mathcal{I}_{K,j}$, $\lambda_{j,\ell}$ denotes the barycentric coordinate of S_j in K_ℓ; $F_{j,\ell}$ denotes the face opposite to vertex S_j in element K_ℓ. We call $\mathcal{S}_{j,\ell}$ the outward normal vector of $F_{j,\ell}$ and of norm $|\mathcal{S}_{j,\ell}| = |F_{j,\ell}|$.
Let's introduce spaces of piecewise regular elements:
We set $\mathcal{P}_h H^1 = \left\{v \in L^2(\Omega)\,; \quad \forall \ell \in \mathcal{I}_K,\, v_{|K_\ell} \in H^1(K_\ell)\right\}$, endowed with the scalar product :

$$(v,w)_h := \sum_{\ell\in\mathcal{I}_K} (\mathbf{grad}\, v, \mathbf{grad}\, w)_{\mathbf{L}^2(K_\ell)} \quad \|v\|_h^2 = \sum_{\ell\in\mathcal{I}_K} \|\mathbf{grad}\, v\|^2_{\mathbf{L}^2(K_\ell)}.$$

We set $\mathcal{P}_h\mathbf{H}^1 = [\mathcal{P}_h H^1]^d$, endowed with the scalar product :

$$(\mathbf{v},\mathbf{w})_h := \sum_{\ell\in\mathcal{I}_K} (\mathbf{Grad}\, \mathbf{v}, \mathbf{Grad}\, \mathbf{w})_{\mathbb{L}^2(K_\ell)} \quad \|\mathbf{v}\|_h^2 = \sum_{\ell\in\mathcal{I}_K} \|\mathbf{Grad}\, \mathbf{v}\|^2_{\mathbb{L}^2(K_\ell)}.$$

Let $f \in \mathcal{I}_F^i$ such that $F_f = \partial K_L \cap \partial K_R$ and let $\mathbf{n}_f$ the unit normal that is outward K_L oriented.
The jump of a function $v \in \mathcal{P}_h H^1$ across the facet F_f, in $\mathbf{n}_f$ direction, is defined as follows: $[v]_{F_f} := v_{|K_L} - v_{|K_R}$. For $f \in \mathcal{I}_F^b$, we set: $[v]_{F_f} := v_{|F_f}$.
We set $\mathcal{P}_h\mathbf{H}(\mathrm{div}\,) = \left\{\mathbf{v} \in \mathbf{L}^2(\Omega)\,; \quad \forall \ell \in \mathcal{I}_K,\, \mathbf{v}_{|K_\ell} \in \mathbf{H}(\mathrm{div}\,; K_\ell)\right\}$, and we define the operator $\mathrm{div_h}$ such that:

$$\forall \mathbf{v} \in \mathcal{P}_h\mathbf{H}(\mathrm{div}\,),\, \forall q \in L^2(\Omega), \quad (\mathrm{div_h}\, \mathbf{v}, q) = \sum_{\ell\in\mathcal{I}_K} (\mathrm{div}\, \mathbf{v}, q)_{L^2(K_\ell)}.$$

For all $D \subset \mathbb{R}^d$, and $k \in \mathbb{N}^*$, we call $P^k(D)$ the set of order k polynomials on D, $\mathbf{P}^k(D) = (P^k(D))^d$, and we consider the space of the broken polynomials:

$$P^k_{disc}(\mathcal{T}_h) = \left\{q \in L^2(\Omega); \quad \forall \ell \in \mathcal{I}_K,\, q_{|K_\ell} \in P^k(K_\ell)\right\}, \quad \mathbf{P}^k_{disc}(\mathcal{T}_h) := (P^k_{disc}(\mathcal{T}_h))^d.$$

We let $P^0(\mathcal{T}_h)$ be the space of piecewise constant functions on $\mathcal{T}_h$. For all $k \in \mathbb{N}$, we consider the space $Q_{k,h}$ such that:

$$Q_{k,h} := P^k(\mathcal{T}_h\,) \cap L^2_{zmv}(\Omega). \tag{8}$$

We will now describe three numerical schemes to solve (2) for which the components of the velocity is discretized with the first order nonconforming Crouzeix-Raviart finite element method [8, §5, Example 4]. For simplicity, we suppose now that $\mathbf{f} \in \mathbf{L}^2(\Omega)$.

3. The $\mathbf{P}^1_{nc} - P^0$cheme

The first order nonconforming finite element method was introduced by Crouzeix and Raviart in the seminal paper [8] to solve Stokes Problem (2). We call it the $\mathbf{P}^1_{nc} - P^0$ scheme. Let us consider X_h (resp. $X_{0,h}$), the space of nonconforming approximation of $H^1(\Omega)$ (resp. $H^1_0(\Omega)$) of order 1:

$$X_h = \left\{v_h \in P^1_{disc}(\mathcal{T}_h)\,; \quad \forall f \in \mathcal{I}_F^i,\, \int_{F_f} [v_h] = 0\right\}, \tag{9}$$

$$X_{0,h} = \left\{v_h \in X_h\,; \quad \forall f \in \mathcal{I}_F^b,\, \int_{F_f} [v_h] = 0\right\}. \tag{10}$$

The condition on the jumps of v_h on the inner facets is often called the patch-test condition. Due to this condition, one can prove that [8, Lemma 2]:

Proposition 3.1. *The broken norm $v_h \to \|v_h\|_h$ is a norm over $X_{0,h}$.*

The following discrete Poincaré–Steklov inequality holds [9, Lemma 36.6]: there exists a constant $C_{PS}^{nc} > 0$ such that

$$\forall v_h \in X_{0,h}, \quad \|v_h\|_{L^2(\Omega)} \leq C_{PS}^{nc} \, \|v_h\|_h. \tag{11}$$

The constant C_{PS}^{nc} is independent of the triangulation $\mathcal{T}_h$ and it is proportional to the diameter of Ω.
We can endow $X_{0,h}$ with the basis $(\psi_f)_{f \in \mathcal{I}_F^i}$ such that: $\forall \ell \in \mathcal{I}_K$,

$$\psi_{f|K_\ell} = \begin{cases} 1 - d\lambda_{i,\ell} & \text{if } f \in \mathcal{I}_{F,\ell}, \\ 0 & \text{otherwise,} \end{cases}$$

where S_i is the vertex opposite to F_f in K_ℓ. We then have $\psi_{f|F_f} = 1$, so that $[\psi_f]_{F_f} = 0$ if $f \in \mathcal{I}_F^i$ (i.e. $F_f \in \Omega$), and $\forall f' \neq f$, $\int_{F_{f'}} \psi_f = 0$. We have: $X_{0,h} = \text{vect}\left((\psi_f)_{f \in \mathcal{I}_F^i}\right)$.
The Crouzeix-Raviart interpolation operator π_h for scalar functions is defined by:

$$\pi_h : \begin{cases} H^1(\Omega) & \to & X_h \\ v & \mapsto & \displaystyle\sum_{f \in \mathcal{I}_F} \pi_f v \, \psi_f \end{cases}, \text{ where } \pi_f v = \frac{1}{|F_f|} \int_{F_f} v.$$

Notice that $\forall f \in \mathcal{I}_F$, $\int_{F_f} \pi_h v = \int_{F_f} v$. Moreover, the Crouzeix-Raviart interpolation operator preserves the constants, so that $\pi_h \underline{v}_\Omega = \underline{v}_\Omega$ where $\underline{v}_\Omega = \int_\Omega v / |\Omega|$.

The space of nonconforming approximation $\mathbf{H}_0^1(\Omega)$ of order 1 is $\mathbf{X}_{0,h} = (X_{0,h})^d$. For a vector $\mathbf{v} \in \mathbf{H}^1(\Omega)$ of components $(v_{d'})_{d'=1}^d$, the Crouzeix-Raviart interpolation operator is such that: $\Pi_h \mathbf{v} = (\pi_h v_{d'})_{d'=1}^d$. We recall the following result:

Proposition 3.2. *The Crouzeix-Raviart interpolation operator Π_h can play the role of the Fortin operator:*

$$\forall \mathbf{v} \in \mathbf{H}^1(\Omega) \quad \|\Pi_h \mathbf{v}\|_h \leq \|\mathbf{Grad}\, \mathbf{v}\|_{\mathbb{L}^2(\Omega)}, \tag{12}$$

$$\forall \mathbf{v} \in \mathbf{H}^1(\Omega) \quad (\text{div}_\text{h}\, \Pi_h \mathbf{v}, q_h) = (\text{div}\, \mathbf{v}, q_h)_{L^2(\Omega)}, \quad \forall q \in Q_h. \tag{13}$$

Moreover, for all $\mathbf{v} \in \mathbf{P}^1(\Omega)$, $\Pi_h \mathbf{v} = \mathbf{v}$.

Notice that the stability constant of the bound on $\|\Pi_h \mathbf{v}\|_h$ is equal to 1 [1, Lemma 2] : it is independent of the mesh.
Let us set $Q_h = Q_{0,h}$. We now define the following bilinear forms:

$$a_{\nu,h} : \begin{cases} \mathbf{X}_{0,h} \times \mathbf{X}_{0,h} & \to & \mathbb{R} \\ (\mathbf{u}_h', \mathbf{v}_h) & \mapsto & \nu\,(\mathbf{u}_h', \mathbf{v}_h)_h \end{cases} \text{ and } b_h : \begin{cases} \mathbf{X}_{0,h} \times Q_h & \to & \mathbb{R} \\ (\mathbf{v}_h, q_h) & \mapsto & -(\text{div}_\text{h}\, \mathbf{v}_h, q_h) \end{cases}. \tag{14}$$

We suppose here that $\mathbf{f} \in \mathbf{L}^2(\Omega)$. The discretization of variational formulation (6) reads:

$$\text{Find } (\mathbf{u}_h, p_h) \in \mathbf{X}_{0,h} \times Q_h \,|\, \begin{cases} a_{\nu,h}(\mathbf{u}_h, \mathbf{v}_h)_h + b_h(\mathbf{v}_h, p) &=& (\mathbf{f}, \mathbf{v}_h)_{L^2(\Omega)} & \forall \mathbf{v}_h \in \mathbf{X}_{0,h}, \\ b_h(\mathbf{u}_h, q_h) &=& 0 & \forall q_h \in Q_h. \end{cases} \tag{15}$$

This saddle point problem is well-posed. Indeed, the bilinear form $a_{\nu,h}(\cdot,\cdot)$ is continuous and coercive. Moreover, the bilinear form $b_h(\cdot,\cdot)$ is continuous and due to Proposition 1.1 and Proposition 3.2, it satisfies the following discrete inf-sup condition:

$$\forall q_h \in Q_h \backslash \{0\}, \quad \exists\, \mathbf{v}_h \in \mathbf{X}_{0,h} \backslash \{0\} \,|\, \quad \frac{b_h(\mathbf{v}_h, q_h)}{\|\mathbf{v}_h\|_h \, \|q_h\|_{L^2(\Omega)}} \geq C_\text{div}\,. \tag{16}$$

Suppose there exists $\phi \in H^1(\Omega) \cap L^2_{zmv}(\Omega)$ such that $\mathbf{f} = \mathbf{grad}\, \phi$. In that case, the solution to Problem (2) is $(\mathbf{u}, p) = (0, \phi)$. By integrating by parts, we have:

$$\forall \mathbf{v}_h \in \mathbf{X}_{0,h}, \quad (\mathbf{f}, \mathbf{v}_h)_{L^2(\Omega)} = -(\text{div}_\text{h}\, \mathbf{v}_h, \phi) + \sum_{f \in \mathcal{I}_F^i} \int_{F_f} [\mathbf{v}_h \cdot \mathbf{n}_f]\, \phi.$$

The term with the jump acts as a numerical source, which numerical influence is proportional to $1/\nu$. Hence, we cannot obtain exactly $\mathbf{u}_h = 0$. There are different strategies to cure this well-known problem:

- Using a polynomial approximation of higher degree [10, 11].
- Increasing the space of the discrete pressures [12, 13].
- Projecting the test-function on a discrete subspace of $\mathbf{H}(\text{div}\,;\Omega)$ [14].

We propose in the next Section to give details on the second strategy.

4. The $\mathbf{P}^1_{nc} - (P^0 + P^1)$cheme

In his thesis [12], Heib proposed to use the following discrete pressures space (cf. (8)):

$$\widetilde{Q}_h = Q_{0,h} \oplus Q_{1,h}. \tag{17}$$

For any $\widetilde{q}_h \in \widetilde{Q}_h$, we write: $\widetilde{q}_h = q_{0,h} + q_{1,h}$, where $q_{0,h} \in Q_{0,h}$ and $q_{1,h} \in Q_{1,h}$.
Let us consider the following bilinear form:

$$\widetilde{b}_h : \left\{ \begin{array}{lcl} \mathbf{X} \times \widetilde{Q}_h & \to & \mathbb{R} \\ (\mathbf{v}_h, \widetilde{q}_h) & \mapsto & -(\mathrm{div_h}\, \mathbf{v}_h, q_{0,h}) + (\mathbf{v}_h, \mathbf{grad}\, q_{1,h})_{\mathbf{L}^2(\Omega)} \end{array} \right. . \tag{18}$$

The discretization of Problem (6) with $\mathbf{P}^1_{nc} - (P^0 + P^1)$ finite elements reads:

$$\text{Find } (\mathbf{u}_h, p_h) \in \mathbf{X}_{0,h} \times \widetilde{Q}_h \,|\, \left\{ \begin{array}{rcll} a_{\nu,h}(\mathbf{u}_h, \mathbf{v}_h)_h + \widetilde{b}_h(\mathbf{v}_h, p_h) & = & (\mathbf{f}, \mathbf{v}_h)_{L^2(\Omega)} & \forall \mathbf{v}_h \in \mathbf{X}_{0,h}, \\ \widetilde{b}_h(\mathbf{u}_h, \widetilde{q}_h) & = & 0 & \forall \widetilde{q}_h \in \widetilde{Q}_h. \end{array} \right. \tag{19}$$

We will need the following Hypothesis [15, Hyp. 4.1]:

Hypothesis 1. *We suppose that the triangulation $\mathcal{T}_h$ is such that the boundary $\partial\Omega$ contains at most one edge in dimension $d = 2$ and at most two faces in dimension $d = 3$, of the same element K_ℓ, $\ell \in \mathcal{I}_K$.*

Under Hypothesis (1), one can prove that the bilinear form $\widetilde{b}_h(\cdot,\cdot)$ is continuous and that it satisfies the following discrete inf-sup condition [12, §4.2]:

$$\forall \widetilde{q}_h \in \widetilde{Q}_h \backslash \{0\}, \quad \exists\, \mathbf{v}_h \in \mathbf{X}_{0,h} \backslash \{0\} \,|\, \quad \frac{\widetilde{b}_h(\mathbf{v}_h, \widetilde{q}_h)}{\|\mathbf{v}_h\|_h \, \|\widetilde{q}_h\|_{L^2(\Omega)}} \geq \widetilde{C}_{\mathrm{div}}\,, \tag{20}$$

where the constant $\widetilde{C}_{\mathrm{div}}$ is independent of the mesh size. Compared to $\mathbf{P}^1_{nc} - P^0$ scheme, the $\mathbf{P}^1_{nc} - (P^1 + P^0)$ scheme gives a better approximation of the velocity in the sense that the discrete mass conservation equation is strengthened. Indeed, one can show, for $d = 2$ that [13, Theorem 4.3.2]:

Property 1. *Let $\mathbf{v}_h \in \mathbf{V}_h := \{\mathbf{w}_h \in \mathbf{X}_h \,|\quad \forall q_h \in \widetilde{Q}_h, \quad \widetilde{b}_h(\mathbf{w}_h, q_h) = 0\}$.*
Then for $d = 2$, we have: for all $q_{2,h} \in Q_{2,h}$, $\widetilde{b}_h(\mathbf{v}_h, q_{2,h}) = (\mathbf{grad}\, q_{2,h}, \mathbf{v}_h)_{\mathbf{L}^2(\Omega)} = 0$.

The proof of Property 1 relies on a quadrature formula which uses the degrees of freedom of the discrete pressure. As this formula cannot be extended in $3D$, this property does not hold. To recover Property 1 in $3D$, we must introduce P^2 discrete pressure degrees of freedom, located on the edges of the mesh, as detailed in [13]. This increases the number of unknowns by the number of cells, which leads to an expensive linear system. Hence, we look for a numerical scheme which could be as precise in $3D$ than in $2D$, but at a lower cost. In the next Section, we propose a new strategy, which relies on the multi-points flux approximation to discretize the pressure gradient term in (2).

5. The $\mathbf{P}^1_{nc} - P^0_{Mps}$cheme

Here, we use the symmetric MPFA scheme (where MPFA stands for *multi-points flux approximation*) to discretize the pressure gradient term in (2), in the case of a simplicial mesh. This scheme is part of the gradient scheme formalism and the resulting diffusion operator is consistent with the hypothesis given by [16, Theorem 12.5]. The discrete pressure space remains $Q_h = Q_{0,h}$. We call this new scheme the $\mathbf{P}^1_{nc} - P^0_{Mps}$ scheme.

Let us consider the $2D$ case. To design the scheme, as it has been initially done in [4, 17], we start by splitting the triangles into three quadrangles, connecting the barycentre of the triangle to the midpoint of each edges. Considering some $q_h \in Q_h$, we will calculate an affine approximation of Q_h on each quadrangle. To do so, we need to add temporary auxiliary unknowns located on the third of the edges.
Let us introduce some notations.

Let $j \in \mathcal{I}_S$. We define the macro-element $\mathcal{M}_j$ such that $\overline{\mathcal{M}}_j := \bigcup_{\ell \in \mathcal{I}_{K,j}} \overline{K}_\ell$. Let's renumber the vertices so that: $S_0 = S_j$, $\mathcal{I}_{S,0} = \{1, \cdots, N_{S,0}\}$ and for all $i \in \mathcal{I}_{S,0}$, $S_i S_{i+1} \in \mathcal{F}_h$ (setting $S_{N_{S,0}+1} = S_{N_{S,0}}$). For $i \in \mathcal{I}_{S,0}$ we denote by:

- K_i the triangle of vertices $S_0 S_i S_{i+1}$, and we call its barycentre G_i.

- F_i the edge such that $F_i = S_0 S_i$, and we call M_i its midpoint.
- $F_{i,0}$ the edge opposite to S_0 in K_i.
- $\widetilde{F}_i$ the half-edges defined by S_0 and the midpoint of F_i.
- Q_i the quadrangle of vertices $S_0\, M_i\, G_i\, M_{i+1}$ (Fig. 2-(A) for $S_0 \subset \Omega$ and 3-(A) for $S_0 \subset \partial\,\Omega$).

For $i,\, j \in \mathcal{I}_{S,0}$, we denote by $\mathcal{S}_{i,j}$ the normal vector outgoing of K_j at F_i and of norm $|F_i|$. For $i \in \mathcal{I}_{S,0}$, we call $\mathcal{S}_{0,i}$ the normal vector outgoing of K_i at $F_{i,0}$. On Figure 1-(A), we represent $\mathcal{M}_0$ in case $S_0 \subset \Omega$ and $N_{S,0} = 6$. On Figure 1-(B), we represent the triangle K_1 with the vectors $(\mathcal{S}_{j,1})_{j=0}^{2}$ and its barycentre G_1.

(A) Macro-element $\mathcal{M}_0 = S_1\, S_2\, S_3\, S_4\, S_5\, S_6$.

(B) Triangle $K_1 = S_0\, S_1\, S_2$.

FIGURE 1. Notations in case $N_{S,0} = 6$ and $j \in \mathcal{I}_S^i$.

(A) Quadrangles $(Q_i)_{i=1}^{N_{S,0}}$.

(B) Discrete pressures $(\overline{q}_i, \widetilde{q}_i)_{i=1}^{N_{S,0}}$.

FIGURE 2. MPFA Scheme for $j \in \mathcal{I}_S^i$ and $N_{S,0} = 6$.

(A) Quadrangles $(Q_i)_{i=1}^{N_{S,0}}$.

(B) Discrete pressures $(\overline{q}_i, \widetilde{q}_i)_{i=1}^{N_{S,0}}$.

FIGURE 3. MPFA Scheme for $j \in \mathcal{I}_S^b$ and $N_{S,0} = 4$

Let $q_h \in Q_h$. We set $q_{h|K_\ell} := \overline{q}_\ell$.

Consider $S_0 \subset \Omega$ (Fig. 2). Let us build a piecewise affine approximation of q_h on each quadrangle $(Q_i)_{i=1}^{N_{S,0}}$ (see Fig. 2-(B)). We call this approximation $\widetilde{q}_h$. We first introduce auxiliary discrete pressure values $(\widetilde{q}_i)_{i=1}^{N_{S,0}}$

on the thirds of the inner edges of $\mathcal{M}_0$ (see Fig. 2-(b)). For all $j \in \mathcal{I}_{S,i}$, we define $\mathcal{G}_{0,i}(q_h) := \mathbf{grad}\, \widetilde{q}_{h|Q_i}$, using an integration by part as it is done in [4, Sect. 3] and [5, Sect. 1.1.1]:

$$|Q_i|\mathcal{G}_{0,i} = \int_{Q_i} \mathcal{G}_{0,i}(q_h) = \int_{\partial Q_i} \widetilde{q}_h \mathbf{n}_{\partial Q_i} = \widetilde{q}_i \frac{\mathcal{S}_{i,i}}{d} + \widetilde{q}_{i+1} \frac{\mathcal{S}_{i+1,i}}{d} + \overline{q}_i(-\frac{\mathcal{S}_{i,i}}{d} - \frac{\mathcal{S}_{i+1,i}}{d}).$$

Hence, noticing that $|Q_i| = \frac{|T_i|}{d+1}$, we have:

$$\mathcal{G}_{0,i}(q_h) = \frac{1}{|Q_i|}\left((\widetilde{q}_i - \overline{q}_i)\, \frac{\mathcal{S}_{i,i}}{d} + (\widetilde{q}_{i+1} - \overline{q}_i)\, \frac{\mathcal{S}_{i+1,i}}{d} \right) = \frac{d+1}{d\,|T_i|}\left(\widetilde{q}_i\, \mathcal{S}_{i,i} + \widetilde{q}_{i+1}\, \mathcal{S}_{i+1,i} + \overline{q}_i\, \mathcal{S}_{0,i} \right). \tag{21}$$

In order to preserve the flux across the inner edges of $\mathcal{M}_0$, we write that:

$$\forall i \in \mathcal{I}_{S,0}, \quad \mathcal{G}_{0,i}(q_h) \cdot \mathcal{S}_{i+1,i} + \mathcal{G}_{0,i+1}(q_h) \cdot \mathcal{S}_{i+1,i+1} = 0. \tag{22}$$

These $N_{S,0}$ equations with $N_{S,0}$ unknowns (the auxiliary discrete pressure values $(\widetilde{q}_i)_{i=1}^{N_{S,0}}$) lead to a well posed linear system. Thus, we can evaluate the auxiliary discrete pressure values $(\widetilde{q}_i)_{i=1}^{N_{S,0}}$ with the data $(\overline{q}_i)_{i=1}^{N_{S,0}}$. Therefore, we can explicitly express the pressure gradients $(\mathcal{G}_{0,i}(q_h))_{i=1}^{N_{S,0}}$ (21).
Consider now $S_0 \subset \partial\,\Omega$ (see Fig. 3). If $\mathbf{f} \in \mathbf{H}^1(\Omega)$, the solution $(\mathbf{u}, p)$ to Problem (2) is such that:

$$\mathbf{grad}\, p \cdot \mathbf{n}_{|\partial\Omega} = \mathbf{f} \cdot \mathbf{n}_{|\partial\Omega} - \nu \Delta \mathbf{u} \cdot \mathbf{n}_{|\partial\,\Omega}, \tag{23}$$

where $\mathbf{n}_{|\partial\Omega}$ is the unit outward normal vector at $\partial\Omega$.

And we explicit the auxiliary discrete pressure values located on $\partial\,\Omega$ (ie $\widetilde{q}_1$ and $\widetilde{q}_4$ on Fig. 3-(b)) by imposing that for all $i \in \mathcal{I}_{S,0}$ such that $F_i \subset \partial\,\Omega$:

$$\int_{\widetilde{F}_i} \mathcal{G}_{0,i}(q_h) \cdot \mathbf{n}_{|\widetilde{F}_i} = \int_{\widetilde{F}_i} \mathbf{f} \cdot \mathbf{n}_{|\widetilde{F}_i}. \tag{24}$$

These equations are approximations of (23), but seem to give good numerical results as shown in section 6. Again, the auxiliary discrete pressure values solve a well posed linear system. They can be written with the data $(\overline{q}_i)_{i=1}^{N_{S,0}}$ and we can explicitly express $\mathcal{G}_{0,i}(q_h)$.

For $i \in \mathcal{I}_S$, we let $(Q_{i,j})_j \in \mathcal{I}_{S,i}$ be the set of quadrangles built around S_i, and we call $\mathcal{Q}_h$ the mesh of all the quadrangles $\mathcal{Q}_h := (\,(Q_{i,j})_{j\in\mathcal{I}_{S,i}})_{i\in\mathcal{I}_S}$. Let $q_h \in Q_h$ and $i \in \mathcal{I}_S$. In the macro-element $\mathcal{M}_i$, we call $\mathcal{G}_{i,j}(q_h)$ the local reconstructed gradient of q_h. We now define the MPFA gradient reconstruction as the operator $\mathcal{G}_h$:

$$\mathcal{G}_h : \left\{ \begin{array}{ccc} Q_h & \to & \mathbf{P}^0(\mathcal{Q}_h) \\ q_h & \mapsto & \mathcal{G}_h(q_h) \end{array} \right. \quad | \quad \forall i \in \mathcal{I}_S,\, \forall j \in \mathcal{I}_{S,i}, \quad \mathcal{G}_h(q_h)_{|Q_{i,j}} = \mathcal{G}_{i,j}(q_{h|\mathcal{M}_i}). \tag{25}$$

If the data $\mathbf{f}$ is of low regularity, one can enhance the space of discrete pressures, adding the auxiliary unknowns on the boundary as degrees of freedom.
The symmetric MPFA scheme applied to the diffusion operator exhibits some properties:

Proposition 5.1. *The consistent approximation of fluxes in the symmetric MPFA scheme is achieved using triangles and $p \in C^2(\Omega)$. Additionally, exact approximation of gradients for affine functions is obtained by selecting the auxiliary pressure unknowns at the thirds of the edges. Furthermore, the symmetric MPFA scheme exhibits properties of consistency, coercivity, and convergence*

The proof of this proposition can be found in [4, Prop. 2, Prop. 3] and [18, Theorem 3.2].

Let us express our discrete Stokes problem. Let $g_h(\cdot,\cdot)$ be the following bilinear form:

$$g_h : \left\{ \begin{array}{ccc} \mathbf{X}_h \times Q_h & \to & \mathbb{R} \\ (\mathbf{v}_h, q_h) & \mapsto & (\mathcal{G}_h(q_h), \mathbf{v}_h)_{\mathbf{L}^2(\Omega)} \end{array} \right. . \tag{26}$$

The discretization of (2) using the MPFA scheme to discretize the pressure gradient reads:

$$\text{Find } (\mathbf{u}_h, p_h) \in \mathbf{X}_{0,h} \times Q_h \,|\, \left\{ \begin{array}{rcll} a_{\nu,h}(\mathbf{u}_h, \mathbf{v}_h) + g_h(\mathbf{v}_h, p_h) & = & (\mathbf{f}, \mathbf{v}_h)_{\mathbf{L}^2(\Omega)} & \forall \mathbf{v}_h \in \mathbf{X}_h \\ b_h(\mathbf{u}_h, q_h) & = & 0 & \forall q_h \in Q_h \end{array} \right. , \tag{27}$$

where the bilinear forms $a_{\nu,h}(\cdot,\cdot)$ and $b_h(\cdot,\cdot)$ are defined by (14). Notice that the linear system related to variational formulation (27) is not symmetric.

6. Numerical Results on the Stokes Problem

In this Section, we give some $2D$ numerical results which compare the $\mathbf{P}^1_{nc} - P^0_{Mps}$ scheme to the $\mathbf{P}^1_{nc} - P^0$ and $\mathbf{P}^1_{nc} - (P^0 + P^1)$ schemes.
Consider Problem (6) with prescribed solution such that: $(\mathbf{u}, p) = (\mathbf{0}, \varphi)$.
When φ is some affine function, then both $\mathbf{P}^1_{nc} - (P^0 + P^1)$ and $\mathbf{P}^1_{nc} - P^0_{Mps}$ schemes give exactly $\mathbf{u}_h = \mathbf{0}$.
When φ is some quadratic function, then $\mathbf{P}^1_{nc} - (P^0 + P^1)$ scheme gives exactly $\mathbf{u}_h = \mathbf{0}$, as a consequence of Property 1.
In what follows, we set $\Omega = (0,1)^2$. We denote the $L^2(\Omega)$ error estimates of the discrete velocity and pressure by:

$$\varepsilon_0^X(\mathbf{u}_h) := \begin{cases} \|\mathbf{u}_h\|_{\mathbf{L}^2(\Omega)} & \text{if } \mathbf{u} = 0 \\ \dfrac{\|\mathbf{u}_h - \mathbf{u}\|_{\mathbf{L}^2(\Omega)}}{\|\mathbf{u}\|_{\mathbf{L}^2(\Omega)}} & \text{otherwise} \end{cases} \qquad \text{and} \qquad \varepsilon_0^X(p_h) := \frac{\|p_h - p\|_{L^2(\Omega)}}{\|p\|_{L^2(\Omega)}},$$

where: $X = CR$ (resp. $X = Trio$ and $X = Mps$) refers to the solution computed with the $\mathbf{P}^1_{nc} - P^0$ (resp. $\mathbf{P}^1_{nc} - (P^0 + P^1)$ and $\mathbf{P}^1_{nc} - P^0_{Mps}$) scheme.
We first consider Problem (6) with prescribed solution $(\mathbf{u}, p) = (\mathbf{0}, \sin(2\pi x)\,\sin(2\pi y)\,)$. On Fig. 4 (resp. 5), we plot $\varepsilon_0^X(\mathbf{u}_h)$ (resp. $\varepsilon_0^X(p_h)$) against the mesh step h in the logarithmic scale, for $\nu = 1$ and $\nu = 10^{-3}$.

We notice that $\varepsilon_0^X(\mathbf{u}_h) \propto \nu^{-1}$ for the three schemes. Concerning the $\mathbf{P}^1_{nc} - P^0_{Mps}$ scheme, we first remark that $\varepsilon_0^{Mps}(\mathbf{u}_h)$ gives intermediate results between $\varepsilon_0^{CR}(\mathbf{u}_h)$ and $\varepsilon_0^{Trio}(\mathbf{u}_h)$ (see Fig. 4). Second, we notice that $\varepsilon_0^{Mps}(p_h) \approx \varepsilon_0^{Trio}(p_h)$. Finally, we notice that the $\mathbf{P}^1_{nc} - P^0_{Mps}$ scheme returns a convergence rate of order 3 for $\varepsilon_0^{Mps}(\mathbf{u}_h)$ and 2 for $\varepsilon_0^{Mps}(p_h)$.

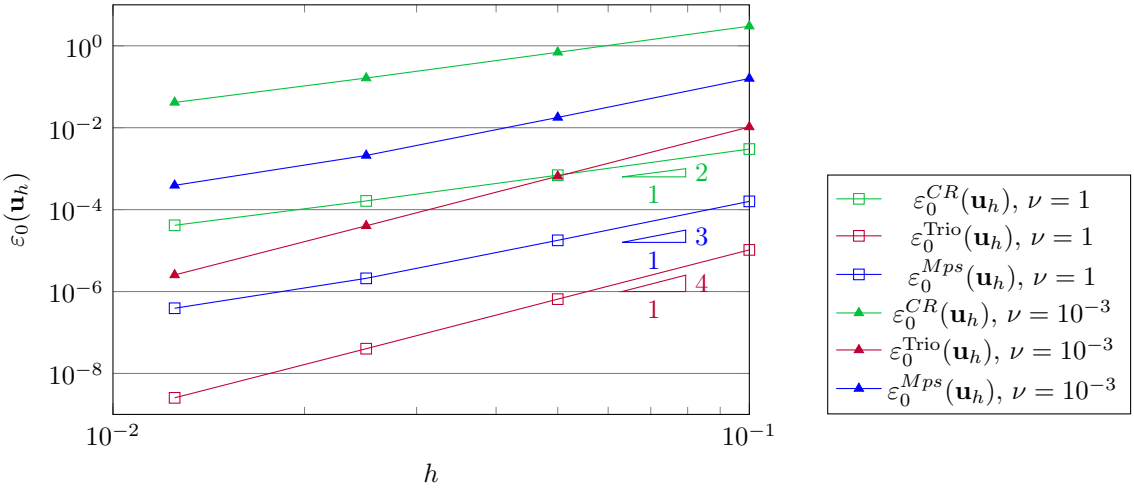

Figure 4. $\varepsilon_0^X(\mathbf{u}_h)$ for $(\mathbf{u}, p) = (\mathbf{0}, \sin(2\pi x)\,\sin(2\pi y)\,)$

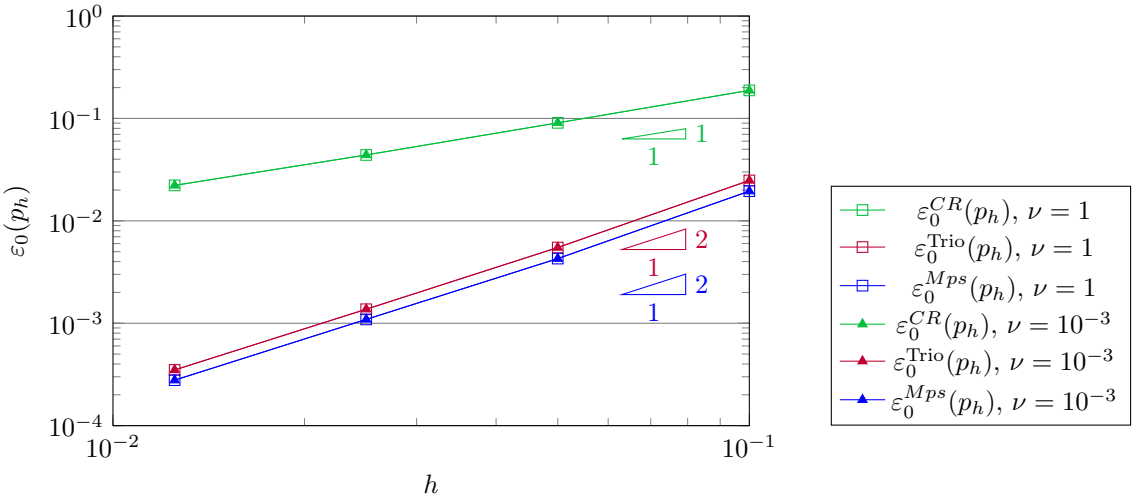

FIGURE 5. $\varepsilon_0(p_h)$ for $(\mathbf{u}, p) = (\mathbf{0}, \sin(2\pi x)\,\sin(2\pi y)\,)$

We notice that, compared to the $\mathbf{P}^1_{nc} - P^0$ scheme, the errors are greatly reduced by the $\mathbf{P}^1_{nc} - (P^0 + P^1)$ and $\mathbf{P}^1_{nc} - P^0_{Mps}$ schemes. These schemes allow to attenuate the amplitude of spurious velocities and hence provide a better simulation. This is illustrated by the resolution of (2) with $(\mathbf{u}, p)$ defined by (28). In this case, as $\mathbf{u}$ is not an affine function, the three schemes return a convergence rate of order 2 for $\varepsilon_0^{Mps}(\mathbf{u}_h)$ and 1 for $\varepsilon_0^{Mps}(p_h)$. The resulting errors for $h = 0.1$ and $h = 0.0125$ are plotted against viscosity in Figures 6 and 7. On these plots, we notice that the $\mathbf{P}^1_{nc} - P^0_{Mps}$ scheme gives intermediate results. We also notice that the spurious velocities errors become overriding when:

- $\nu \leq 10^0$ with $h = 0.1$ and $\nu \leq 10^0$ with $h = 0.0125$ for the $\mathbf{P}^1_{nc} - P^0$.
- $\nu \leq 10^{-2}$ with $h = 0.1$ and $\nu \leq 10^{-3}$ with $h = 0.0125$ for the $\mathbf{P}^1_{nc} - P^0_{Mps}$.
- $\nu \leq 10^{-3}$ with $h = 0.1$ and $\nu \leq 10^{-5}$ with $h = 0.0125$ for the $\mathbf{P}^1_{nc} - (P^0 + P^1)$.

The tipping viscosity point, where the spurious velocities errors become dominant, depends on the velocity error generated by the lack of consistency of the discrete right on side of (27) and therefore the mesh size. As these schemes converge with different orders when $\mathbf{u} = 0$, it can be seen that decreasing the mesh size reduces the viscosity at which this point is reached more or less depending on the order. For the pressure, the L^2-error (plotted in Fig. 7) decreases, with order one, to a threshold value as expected by classical error analysis.

$$(\mathbf{u}, p) = \left(\begin{pmatrix} (\cos(2\pi x) - 1)\,\sin(2\pi y) \\ -(\cos(2\pi y) - 1)\,\sin(2\pi x) \end{pmatrix}, \sin(2\pi x)\sin(2\pi y) \right) \tag{28}$$

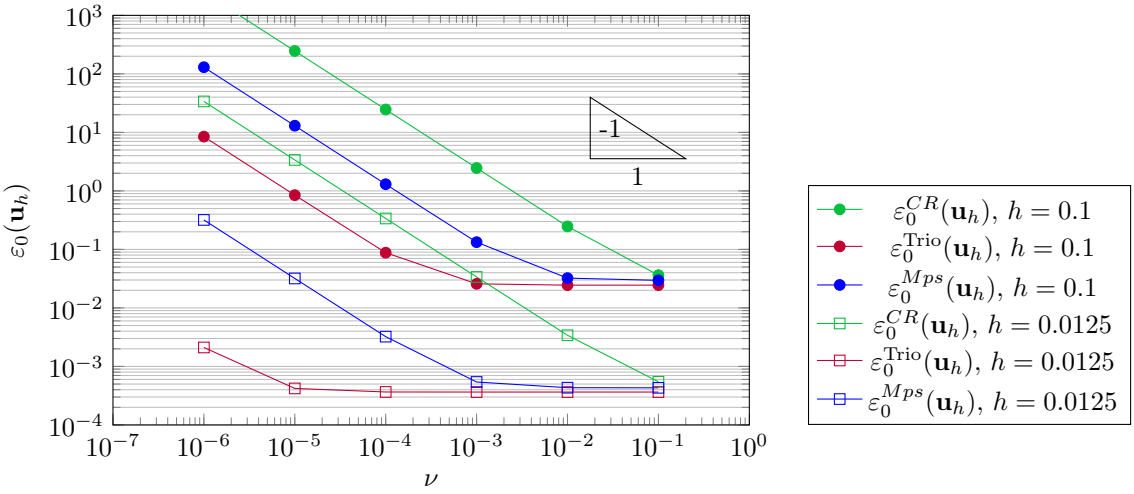

FIGURE 6. $\varepsilon_0(\mathbf{u}_h)$ for $\mathbf{u}$ and p sinusoidal functions against viscosity with different mesh sizes

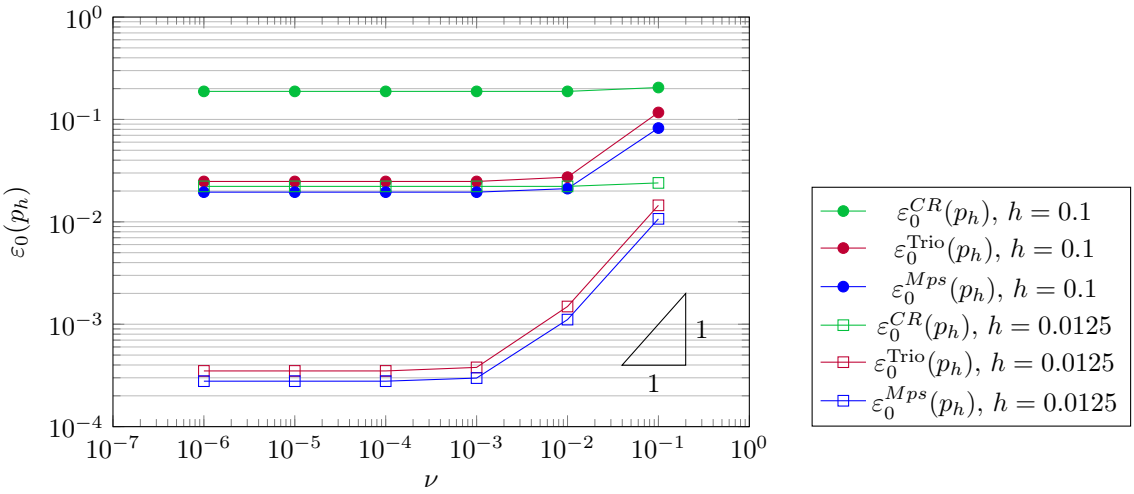

FIGURE 7. $\varepsilon_0(p_h)$ for $\mathbf{u}$ and p sinusoidal functions against viscosity with different mesh sizes

We are also interested in the sensitivity to the mesh deformation. Indeed, nowadays, mesh refinement techniques based on a posteriori error estimators or industrial constraints can generate anisotropic meshes. In this subSection, we show that the three schemes have the same behaviour with respect to the regularity of the mesh. To illustrate this property, we propose to use the Kershaw meshes presented in the benchmark [19] (see Fig. 8) with $(\mathbf{u}, p)$ in (28). As the mesh is composed of quadrilaterals, we cut them with along one of the diagonal, which allows us to remain within reasonable convergence assumptions. The mesh is represented in Fig. 8 and we plot the results in Fig 9 and 10. We can see that the schemes have a convergence rate of order 2 for $\varepsilon_0^X(\mathbf{u}_h)$ and 1 for $\varepsilon_0^X(p_h)$.

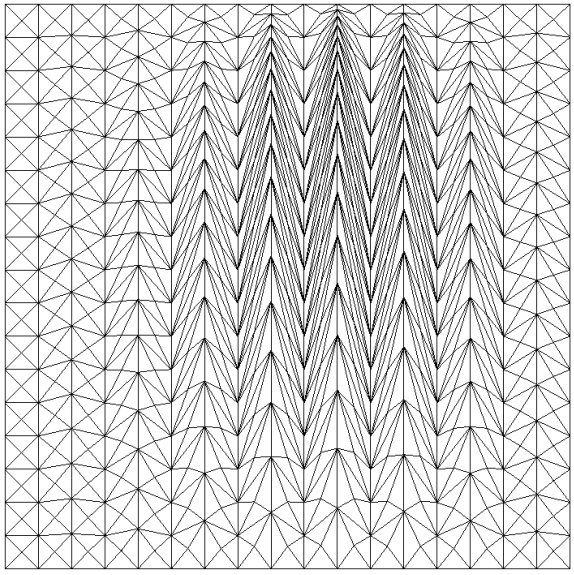

FIGURE 8. Kershaw mesh.

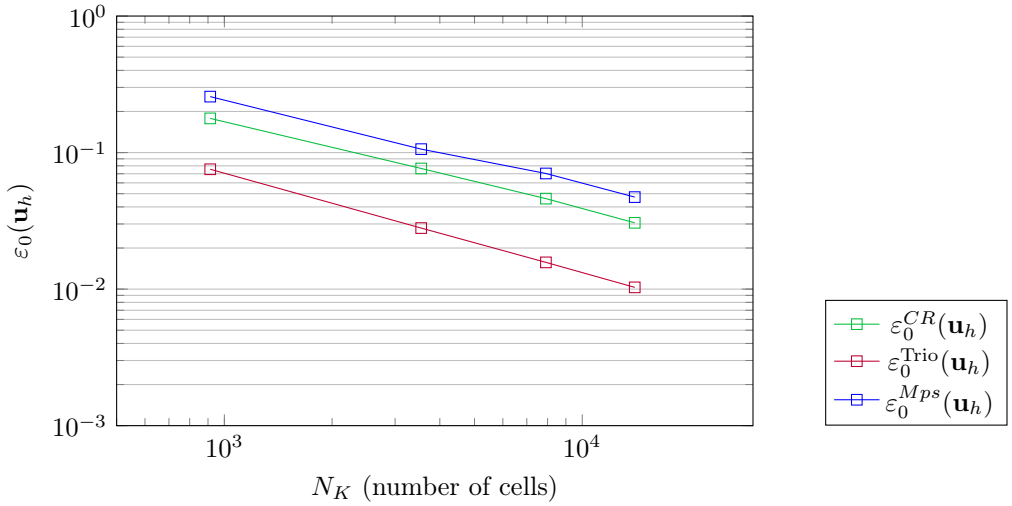

FIGURE 9. $\varepsilon_0(\mathbf{u}_h)$ for $\mathbf{u}$ and p sinusoidal functions against viscosity with different kershaw meshes and $\nu = 1$.

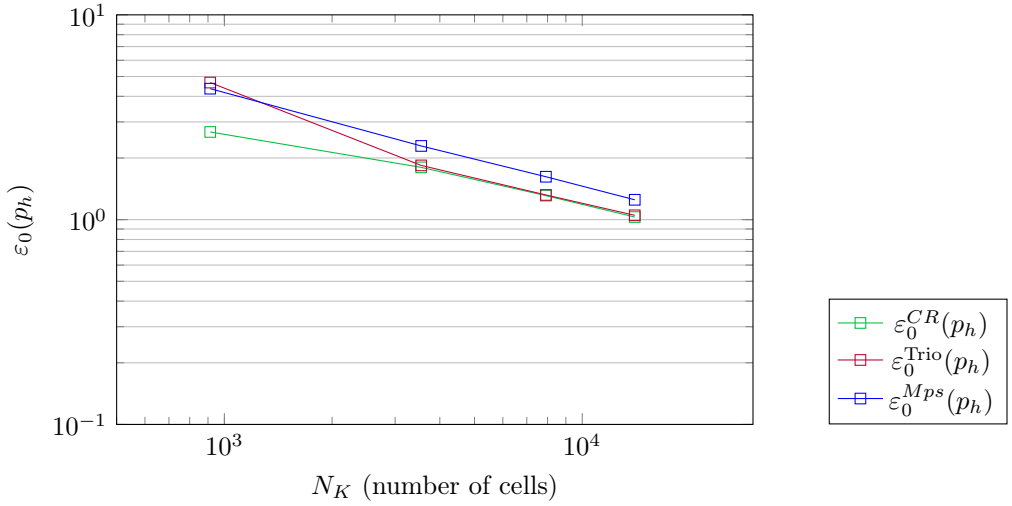

FIGURE 10. $\varepsilon_0(p_h)$ for $\mathbf{u}$ and p sinusoidal functions against viscosity with different kershaw meshes and $\nu = 1$.

7. Numerical Results on the Navier-Stokes Problem

We choose the convection scheme initially presented in [20, Eq. 2.8]. This choice is motivated by the result of the Benchmark [21] where the scheme presents good convergence and stability results without increasing the stencil of the scheme. To resolve efficiently the Navier-Stokes equations, we use a prediction correction time-scheme [22] [23], which consists in calculating a predicted velocity (with non-zero divergence), then solving the pressure at the next time and correcting the velocity to ensure piecewise divergence-free flow. With this approach, the velocity and pressure resolutions are decoupled.

As the approach is not classical, it is interesting to check the convergence of the scheme on Navier-Stokes. This leads to study the Green-Taylor vortex solution which is a well-known analytical solution to (1).

Let first introduce the space-discretization of the Navier-Stokes equations (1) :

$$\begin{cases} M\partial_t U + \nu KU + L(U)U + GP = F \\ DU = 0 \end{cases} \tag{29}$$

where U, P contains the velocity and pressure unknowns and F is the right hand side. The matrices M and K are respectively the mass and stiffness matrices. Also, the matrices G and D represent the gradient and divergence operators. Finally, the matrix $L(U)$ is associated with the convection term and $\partial_t U$ is the time derivative of U.

We first present the prediction-correction time scheme :

(1) Prediction step:

$$M\frac{U^* - U^n}{\delta t} + \nu KU^* + L(U^n)U^n + GP^n = F^n \quad \text{we may have} \quad DU^* \neq 0 \tag{30}$$

(2) Pressure solver step:

$$\delta t(D\widetilde{M}^{-1}G)\delta P = DU^* \tag{31}$$

with $\delta P = P^{n+1} - P^n$

(3) Correction step:

$$U^{n+1} = U^* - \delta t\widetilde{M}^{-1}G\delta P \tag{32}$$

with $\widetilde{M} = M + \delta t\,\nu K$. The CFL of the global system is then:

$$\delta t < Ch \tag{33}$$

In Equation (31), even if the system is symmetric positive definite, the matrix $D\widetilde{M}^{-1}G$ is dense so we cannot store it. We would need a $2-$level iterative solver for the Pressure solver step.

Remark 7.1. (*Projection scheme*):
We can approximate $\widetilde{M}$ by M following the ideas of [22]. Indeed, the matrix M is diagonal in $2D$ and in $3D$ it is equivalent to a diagonal matrix. In that case, the matrix $D\widetilde{M}^{-1}G$ is sparse and can be built explicitly. This leads to a linear system that is faster to solve but less accurate. This approximation is the one currently used in the TrioCFD code. In a second step, Although the MPFA scheme leads to a non-symmetrical resolution, an approximation of (31) with $\widetilde{M} = M$ can correct this. The system is equivalent to a diffusion problem, and if we uniformize the mass matrix by approaching M by mId, where Id denotes the identity matrix and m the minimum volume of $T \in \mathcal{T}_h$, we recover a system close to the classical MPFA symmetric system for the Laplacian problem [4]. The idea is to substitute this system with the classical MPFA one.

Remark 7.2. (*Parallelization I*):
To obtain a massive parallelization of the code, we use a ghost cells method (see Fig. 11) by storing the neighbors' unknowns of the pressure of a domain handled by one processor. By doing that, the communication is highly reduced and the sub-problems are almost uncoupled. The First step is to solve (30). As everything is explicit, U^* can be calculated even on the border of two processor's domains due to the stencil of the scheme and the storage of U^n and P^n, then (31) can be resolved. The next part is where the processors need to communicate, updating the pressure unknowns located on the ghost cells. Finally, (32) is given by an explicit computation.

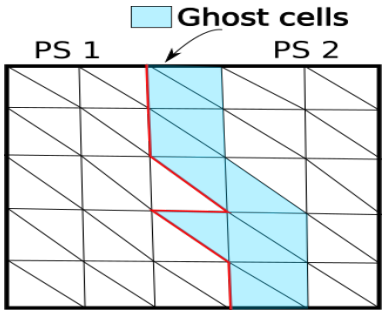

FIGURE 11. Ghost cells for processor 1 located on the domain of processor 2. The border is marked in red.

Remark 7.3. (*Parallelization II*):
An interesting aspect of the new method is the parallelization. Indeed, the matrices obtained with (22) can be constructed independently. Also, the same method detailed in the previous remark can be applied to the $\mathbf{P}^1_{nc} - P^0_{Mps}$ scheme.

Remark 7.4. (*Natural boundary condition for the pressure*):
As we did in Section 6, to determine the auxiliary pressures on the boundary of the MPFA scheme, we impose

a condition for the pressure gradient at the edge. On each half-edge $\widetilde{F}_i$ related to the vertex S_0 and edge $F_i \in \partial\Omega$:

$$\int_{\widetilde{F}_i} \mathcal{G}_{0,i} \cdot \mathbf{n}_{|\widetilde{F}_i} = \int_{\widetilde{F}_i} (\mathbf{f} + (\mathbf{u}_h^{n+1} - \mathbf{u}_h^n)/\delta t + (\mathbf{u}_h^n \cdot \mathbf{grad}\,)\mathbf{u}_h^n) \cdot \mathbf{n}_{|\widetilde{F}_i}. \tag{34}$$

Let $\Omega = (0,1)^2$. We prescribe the solution to Equation (1) with $\mathbf{f} = \mathbf{0}$, to be:

$$\left\{ \begin{array}{rcl} \mathbf{u} & = & \begin{pmatrix} -\cos(2\pi(x+\frac{1}{2}))\sin(2\pi(y+\frac{1}{2}))exp(-8\pi^2 t) \\ \sin(2\pi(x+\frac{1}{2}))\cos(2\pi(y+\frac{1}{2}))exp(-8\pi^2 t) \end{pmatrix} \\ p & = & -\frac{1}{4}\cos(4\pi(x+\frac{1}{4})) + \cos(4\pi(y+\frac{1}{2}))\, exp(-16\pi^2 t) \end{array} \right. \tag{35}$$

We set $t_{max} = 0.01$ the final time of the simulation. The time step is chosen with respect to the CFL (33) with $C = \frac{1}{2}$. The errors in velocity and pressure at the final time are plotted in Figures 12 and 13 against the mesh step. We can see that the three schemes converge with order 2 for $\varepsilon_0^{Mps}(\mathbf{u}_h)$ and 1 for $\varepsilon_0^{Mps}(p_h)$ as expected.

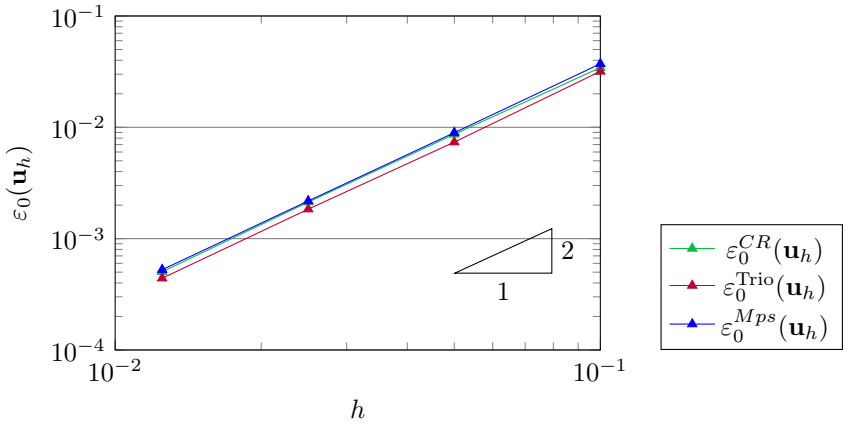

FIGURE 12. $\varepsilon_0(\mathbf{u}_h)$ for $(\mathbf{u}, p) \in (35)$ with $\nu = 1$.

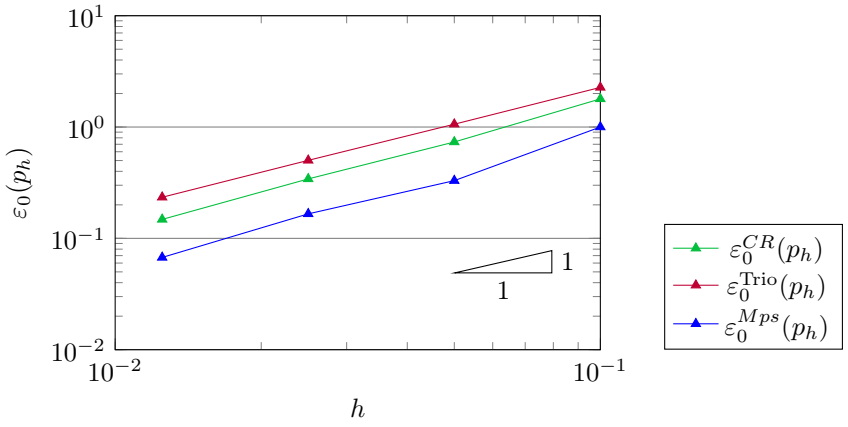

FIGURE 13. $\varepsilon_0(p_h)$ for $(\mathbf{u}, p) \in (35)$ with $\nu = 1$.

8. Conclusion and perspectives

The purpose of this work is to present a new discretization for the gradient of pressure. This scheme presents similar result to $\mathbf{P}^1_{nc} - (P^0 + P^1)$ discretization. However, some points have been left out of the scope of this work and deserve further investigation:

- On the boundary, the continuity of the gradient flows can not be applied. We need boundary conditions to complete the system of elimination of the auxiliary unknowns (22). If the problem has, for the pressure:
  - Dirichlet boundary condition: we can evaluate the value of the auxiliary unknowns on the boundary.
  - Neumann boundary condition: we can evaluate the value of normal component of the pressure gradient on the boundary.

  Otherwise, we can keep the auxiliary unknowns and complete the problem with other equations.

- The Section 3 shows that our scheme provides a benefit to the classic $\mathbf{P}^1_{nc} - P^0$ discretization but $\mathbf{P}^1_{nc} - (P^0 + P^1)$ has an additional superconvergence case. This property disappears in 3D, unless we add pressure degrees of freedom on edges which turns out to be costly in computer memory. In that case, the MPFA scheme and $\mathbf{P}^1_{nc} - (P^0 + P^1)$ give comparable results but with a duality between scheme stencil and memory footprint. A study will be carried out to compare the efficiency of the two schemes.
- The scheme seems numerically stable but the inf-sup condition has still not been proven.
- The scheme is currently in development in the CEA thermohydraulic code TrioCFD and its implementation will allow to realize more test.
- The Finite Element Cell-Centered (FECC) scheme is an other gradient discretization scheme, which has similar properties to the MPFA scheme and can handle more general meshes [24]. The same approach can be used to develop a new scheme on polyhedral meshes for the Navier-Stokes problem.

9. Acknowledgements

First, thank you to the organizers of "New Trends in Complex Flows" for allowing us to publish this work. We are grateful to the reviewer for having done careful proofreading. We also want to thank R. Eymard for his involvement in this work. Finally, we acknowledge the CEA SIMU/SITHY project, which funded this work.

References

[1] T. Apel, S. Nicaise, and J. Schöberl. "Crouzeix-Raviart Type Finite Elements on Anisotropic Meshes". In: *Numerische Mathematik* 89.2 (2001). URL, pp. 193–223.

[2] T. Apel, S. Nicaise, and J. Schöberl. "A Non-Conforming Finite Element Method with Anisotropic Mesh Grading for the Stokes Problem in Domains with Edges". In: *IMA Journal of Numerical Analysis* 21 (2001). URL.

[3] L. Agelas and R. Masson. "Convergence of the finite volume MPFA O scheme for heterogeneous anisotropic diffusion problems on general meshes". In: *Acad. Sci. Paris, Ser. I 346* (2008). URL.

[4] C. Le Potier. "A finite volume method for the approximation of highly anisotropic diffusion operators on unstructured meshes". In: *Finite Volumes for Complex Applications IV, Marrakesh, Marocco* (2005). URL.

[5] C. Le Potier. "Construction et développement de nouveaux schémas pour des problèmes elliptiques ou paraboliques". URL. Habilitation à diriger des recherches. Université Paris-Est, 2017.

[6] P.-E. Angeli, M.-A. Puscas, G. Fauchet, and A. Cartalade. "FVCA8 benchmark for the Stokes and Navier-Stokes equations with the TrioCFD code". In: *Finite Volumes for Complex Applications VIII - Methods and Theoretical Aspects*. Ed. by C. Cancès and P. Omnes. Vol. 199. URL. Springer Proceedings in Mathematics & Statistics, 2017, pp. 181–302.

[7] V. Girault and P.-A. Raviart. *Finite element methods for Navier-Stokes equations*. DOI. Springer-Verlag, 1986.

[8] M. Crouzeix and P.-A. Raviart. "Conforming and nonconforming finite element methods for solving the stationary Stokes equations". In: *RAIRO, Sér. Anal. Numer.* 33 (1973). DOI.

[9] A. Ern and J. -L. Guermond. *Finite Elements II: Galerkin approximation, elliptic and mixed PDEs*. URL. Springer, 2021.

[10] M. Fortin and M. Soulie. “A non-conforming piecewise quadratic finite element on triangles”. In: *International Journal for Numerical Methods in Engineering* 19 (1983). URL, pp. 505–520.
[11] E. Jamelot. “Improved stability estimates for solving Stokes problem with Fortin-Soulie finite elements”. cea-03833616. 2023.
[12] S. Heib. “Nouvelles discrétisations non structurées pour des écoulements de fluides à incompressibilité renforcée”. URL. PhD thesis. Université Paris VI, 2003.
[13] T. Fortin. “Une méthode éléments finis à décompositoin L^2 d’ordre élevé motivée par la simulation d’écoulement diphasique bas Mach”. PhD thesis. Université Pierre et Marie Curie – Paris VI, 2006.
[14] A. Linke. “On the Role of the Helmholtz-Decomposition in Mixed Methods for Incompressible Flows and a New Variational Crime”. In: *Comput. Methods Appl. Mech. Engrg.* 268.1 (2014), pp. 782–800.
[15] C. Bernardi and F. Hecht. “More pressure in the finite element discretization of the Stokes problem”. In: *ESAIM: M2AN* 34.5 (2000). DOI, pp. 953–980.
[16] J. Droniou, R. Eymard, T. Gallouet, C. Guichard, and R. Herbin. “The Multi-point Flux Approximation MPFA-O Scheme”. In: URL. The Gradient Discretisation Method, 2018, pp. 343–351.
[17] C. Le Potier. “Schéma volumes finis pour des opérateurs de diffusion fortement anisotropes sur des maillages non structurés”. In: *Comptes Rendus Mathematique Acad. Sci. Paris* (2005). URL.
[18] K. Lipnikov, M. Shashkov, and I. Yotov. “Local flux mimetic finite difference methods”. In: *Numerische Mathematik* 112 (2009). URL, pp. 115–152.
[19] R. Herbin and F. Hubert. “Benchmark on Discretization Schemes for Anisotropic Diffusion Problems on General Grids”. In: *Finite volumes for complex applications V*. hal-00429843. Wiley, 2008, pp. 659–692.
[20] L. Gastaldo, R. Herbin, and J.-C. Latché. “An unconditionally stable finite element-finite volume pressure correction scheme for the drift-flux model”. In: *ESAIM: Mathematical Modelling and Numerical Analysis - Modélisation Mathématique et Analyse Numérique* 44.2 (2010). URL, pp. 251–287.
[21] R. Eymard, P. Feron, and C. Guichard. “Family of convergent numerical schemes for the incompressible Navier-Stokes equations”. In: *Mathematics and Computers in Simulation* 144 (2018). URL, pp. 196–218. ISSN: 0378-4754.
[22] A. Chorin. “A numerical method for solving incompressible viscous flow problems”. In: *Courant Institute of Mathematical Sciences, New York University* 10012 (1967). URL.
[23] R. Temam. “Une méthode d’approximation de la solution des équations de Navier-Stokes”. In: *Bulletin de la Société Mathématique de France* 96 (1968). URL, pp. 115–152.
[24] C. Le Potier and T. H. Ong. “A Cell-Centered Scheme For Heterogeneous Anisotropic Diffusion Problems On General Meshes”. In: *International Journal on Finite Volumes* (2012). URL.